Vibrationally resolved molecular-frame angular distribution of O 1s photoelectrons from CO2 molecules

著者	Saito N., Liu X.-J., Morishita Y., Prumper G., Machida M., Oura M., Yamaoka H., Tamenori Y., Koyano I., Suzuki I. H., Ueda K.
journal or publication title	Physical Review. A
volume	72
number	4
page range	042717
year	2005
URL	http://hdl.handle.net/10097/53546

doi: 10.1103/PhysRevA.72.042717

Vibrationally resolved molecular-frame angular distribution of O 1*s* photoelectrons from CO_2 molecules

N. Saito,[1] X-J. Liu,[2] Y. Morishita,[1] G. Prümper,[2] M. Machida,[3,4] M. Oura,[4] H. Yamaoka,[4] Y. Tamenori,[5] I. Koyano,[3] I. H. Suzuki,[1] and K. Ueda[2,*]

[1]*NMIJ, Institute of Advanced Industrial Science and Technology (AIST), Tsukuba 305-8568, Japan*

[2]*Institute of Multidisciplinary Research for Advanced Materials, Tohoku University, Sendai 980-8577, Japan*

[3]*Department of Material Science, Himeji Institute of Technology, Kamigori, Hyogo 678-1297, Japan*

[4]*RIKEN, Harima Institute, Sayo, Hyogo 679-5148, Japan*

[5]*Japan Synchrotron Radiation Research Institute, Sayo, Hyogo 679-5198, Japan*

(Received 15 May 2005; published 27 October 2005)

Vibrationally resolved O 1*s* photoelectron angular distributions from CO_2 molecules, aligned parallel and perpendicular to the electric vector of the incident light, have been measured in the $5\sigma_g^*$ shape resonance region, with photon energies up to 2 eV above the O 1*s* ionization threshold, using multiple-coincidence electron-ion momentum imaging spectroscopy. The angular distributions depend on the vibrational quanta of the antisymmetric vibrations in the O 1*s* ionized state but do not vary significantly as a function of the photon energy across the $5\sigma_g^*$ shape resonance.

DOI: 10.1103/PhysRevA.72.042717 PACS number(s): 33.80.Eh, 33.60.Fy, 33.20.Tp, 33.20.Rm

Shape resonances that appear in absorption spectra of small molecules above the ionization threshold are usually described as the transition of an electron to an unoccupied molecular valence-like orbital [1] or a temporary trap of the photoelectron by the molecular potential barrier [2]. Dehmer *et al.* predicted that the energy of the shape resonance depends on the internuclear distance and, thus, on the vibrational states of the residual ion core because the characteristic internuclear distance at the time of photoionization varies as a function of vibrational quanta v' [3]. They used valence photoionization of nitrogen molecules N_2 as a typical showcase example.

Because of the advances in soft x-ray monochromators, nowadays, one can measure vibrationally resolved core-level photoemission as a function of photon energy and, thus, the shape resonance energy as a function of vibrational quantum numbers. CO is a well-studied example of the vibrational dependence of the shape resonance energies. The σ^* shape resonances observed in x-ray absorption spectra above both the C 1*s* and O 1*s* thresholds are also present in the C 1*s* and O 1*s* single hole ionization (SHI) cross sections for the individual vibrational components v' and the energy of the v'-resolved shape resonance moves close to the C 1*s* threshold and away from the O 1*s* threshold with an increase in v' [4–6]. This site-selective v' dependence of the resonance energy was interpreted as the variation of characteristic internuclear distances for different vibrational components of C 1*s* and O 1*s* ionized states [5].

As demonstrated by many authors both experimentally and theoretically, one can gain further insight for the photoionization dynamics in molecules by measuring the molecular-frame photoelectron angular distributions (MF-PADs) (see, for example, [7–13]). MF-PADs can be measured in the coincidence experiment detecting the photoelectron and the corresponding ion momentum. In most of the measurements for the MF-PADs reported so far, vibrational components of the final ionic state are not resolved. To discuss the shape resonance phenomena, however, it is indispensable to resolve the vibrational structure, as illustrated in the vibrationally resolved core-level photoemission study [4–6]. Very recently, two groups succeeded in measuring vibrationally resolved MF-PADs for C 1*s* emission from the CO molecule [14,15]. The MF-PADs indeed turned out to depend strongly on the vibrational quantum numbers.

It is interesting to extend these measurements to triatomic molecules in order to explore dynamical features that may arise in MF-PADs for systems beyond CO. In this paper, we report the measurement for vibrationally resolved MF-PADs for O 1*s* photoemission from CO_2 molecules. The O 1*s* orbitals consist of symmetry-adapted molecular orbitals $1\sigma_g$ and $1\sigma_u$. The O 1*s* ionization threshold is at 541.254 eV [16]. In the O 1*s* absorption spectrum, two shape resonances, $1\sigma_u \rightarrow 5\sigma_g^*$ and $1\sigma_g \rightarrow 4\sigma_u^*$, appear at ~542 eV, very close to the O 1*s* ionization threshold, and at ~559 eV, ~18 eV above O 1*s* ionization threshold, respectively [17]. It is worth noting that in the C 1*s* absorption spectrum only the $2\sigma_g \rightarrow 4\sigma_u^*$ shape resonance appears because of symmetry reasons. The $4\sigma_u^*$ shape resonances in the C 1*s* and O 1*s* ionization regions were investigated using vibrationally resolved photoelectron spectroscopy [18,19]. MF-PADs for C 1*s* and O 1*s* photoemission in the $4\sigma_u^*$ shape resonance regions were investigated without vibrational resolution [11,20–22]: no measurements for MF-PADs with vibrational resolution have been reported. Furthermore, no measurements for vibrationally resolved photoelectron spectroscopy have been reported in the region of the $1\sigma_u \rightarrow 5\sigma_g^*$ shape resonance: the kinetic energy of the photoelectron at this resonance is only ~1.2 eV and, therefore, very difficult to measure.

In the present paper, we report on vibrationally resolved MF-PADs for O 1*s* photoemission from CO_2 in the vicinity

*Corresponding author. Electronic address: ueda@tagen.tohoku.ac.jp

of the $5\sigma_g^*$ shape resonance with kinetic energies up to ~2 eV. The experimental method employed here is electron-ion coincidence momentum imaging. The resolution of this method has been improved during the last few years and now one can measure vibrationally resolved MF-PADs [15,23]. This technique has the advantage to detect low-energy electrons without suffering from rapid changes of the transmission function and correction efficiency as a function of kinetic energy.

The experiments were carried out on the *c* branch of the soft x-ray photochemistry beam line 27SU [24] at SPring-8. A figure-8 undulator of this beam line provides linearly polarized light, whose polarization vector E can be horizontal or vertical. With the small front-end-slit used in this experiment, only the central part of the photon beam is used. Therefore the degree of the linear polarization is greater than 99%. The measurements were performed with the vertical direction of the E vector and the photon bandwidth of ~100 meV at a photon energy of ~540 eV. The photon beam, focused to a size of less than 0.2 mm in height and 0.5 mm in width, crosses a supersonic molecular beam of CO_2: the molecular beam is vertical and, thus, coincides with the direction of the E vector.

Our electron-ion coincidence momentum imaging apparatus is based on the measurement of the electron and ion time-of-flight (TOF) with multihit, two-dimensional position sensitive detectors [23,25]. The two TOF spectrometers, a longer one for electrons and a shorter one for ions, are placed face to face. Measurements of the position and the arrival time on the particle detectors (x,y,t) allowed us to extract information about the linear momentum (p_x,p_y,p_z) for each particle without any ambiguity. The TOF spectrometer axis is horizontal and perpendicular to both the photon beam and the E vector (or the molecular beam). The lengths of the acceleration region and the drift region of the electron spectrometer are 32.9 mm and 66.7 mm, respectively. For the ion spectrometer, the length of the acceleration region is 21.6 mm and no drift region is provided. Each of the TOF spectrometers is equipped with a multihit, position-sensitive delay-line detector of the effective diameter of 80 mm [26]. The static extraction field was set to ~0.6 V/mm. A uniform magnetic field was superimposed to the spectrometer by a set of Helmholtz coils outside the vacuum chamber. The magnetic field was set to be 2.8 or 3.2 G. Under these conditions, all the O 1*s* photoelectrons ejected in 4π sr, up to ~2 eV in kinetic energy, were accelerated onto the microchannel plate (MCP) detector.

The storage ring was operated in 6/42 filling +35 bunch mode, which corresponded to a bunch separation of 114 ns. The times of flight of ions and electrons were measured with respect to the bunch marker of the synchrotron radiation source using ultrafast, multihit time-to-digital converters [(TDCs) c027, Hoshin Electronics Co. Ltd.] [23]. These TDCs have a timing resolution of about 120 ps, a multihit capability of 6 events, and the time span of 40 μs. The events were recorded only when at least one electron and two ions were detected in coincidence.

O 1*s* photoemission from a CO_2 molecule leads through Auger decay to the creation of the doubly charged molecule which dissociates into two fragment ions. In our study, we have selected reaction channels in which the molecule fragmented into two ions, $O^+ + CO^+$: the two ions were detected in coincidence. We found that the distribution of the kinetic energy release (KER) of this channel has a wide energy distribution between 3 and 15 eV with its maximum at ~6 eV. With the employed extraction field of 6 V/mm, all the ions ejected in 4π sr up to $R_{KE} \sim 20$ eV can be collected without any discrimination. The ion anisotropy parameter β turned out to be the same (~0.7) for the events with $3 < R_{KE} < 15$ eV and those with $10 < R_{KE} < 15$ eV. This agreement suggests that the axial recoil approximation is valid for all the events with $R_{KE} > 3$ eV. Thus, we used all the O^+ and CO^+ coincidence events ($3 < R_{KE} < 15$ eV) in the analysis described below.

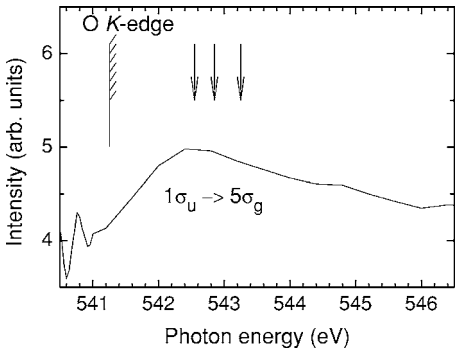

FIG. 1. Total ion yield spectrum of CO_2 in the $1\sigma_u \rightarrow 5\sigma_g$ shape resonance region.

Figure 1 shows the total ion yield spectrum. We have carried out the measurements at three different photon energies indicated by arrows in the figure: 542.55, 542.85, and 543.25 eV. The first energy 542.55 eV corresponds to the energy at which the O 1*s* $1\sigma_u \rightarrow 5\sigma_g$ shape resonance appears in the total ion yield (TIY) spectrum. The energy difference between the first two points, 542.55 and 542.85 eV, corresponds to the spacing of the antisymmetric vibrations (v_3) in the O 1*s* ionized state [27]. The last energy 543.25 eV is at the high-energy shoulder of the shape resonance.

In the present analysis, we selected the events in which ions and electrons are both in the plane perpendicular to the TOF spectrometer axis. This plane includes also the polarization vector E. To select the Σ channel, we have selected the events in which the molecular orientation is parallel to the E vector: the angle between the molecular axis and the E vector is smaller than 21.5°. To select the Π channel, we have selected the events in which the molecular orientation is parallel (<21.5°) to the vector perpendicular to both the E vector and the TOF spectrometer axis. The angle between the momentum of the photoelectron and the TOF spectrometer axis was restricted to be between 78.5° and 101.5°. The selection of this photoelectron direction improves the electron energy resolution because the position resolution is better than the time resolution under the present condition.

Figures 2(a) and 2(b) show the kinetic energy distributions of the O 1*s* photoelectron measured in coincidence with O^+ and CO^+, whose momenta are parallel (Σ) and perpendicular (Π) to the E vector, at a photon energy of 542.55 eV. The dots denote the experimental data obtained from the

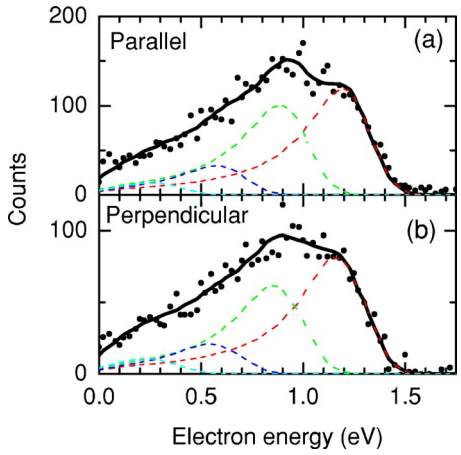

FIG. 2. (Color online) O 1*s* photoelectron spectra of CO_2 measured in coincidence with O^+ and CO^+, whose momenta are (a) parallel (Σ) and (b) perpendicular (Π) to the E vector, respectively, at a photon energy of 542.55 eV. The thick lines are the results of the fitting while the thin dashed lines are the individual vibrational components (see text).

above procedure. We can see the vibrational progression of the antisymmetric stretching mode (v_3). We have fitted the spectra with vibrational progressions with a spacing of 307 meV for the v_3 mode [27]. A post-collision interaction (PCI) line shape by van der Straten *et al.* [28] with a constant natural width of 165 meV [27] was employed for each vibrational component. The thin dashed curves correspond to the vibrational components obtained by the curve fit and the thick curves denote the sum over the vibrational components.

Figure 3 shows the polar plots' vibrationally resolved MF-PAD for O 1*s* photoemission from CO_2 aligned parallel (Σ) and perpendicular (Π) to the E vector measured at the three photon energies, where the polar angle θ is between the photoelectron momentum and the molecular axis. Note that the

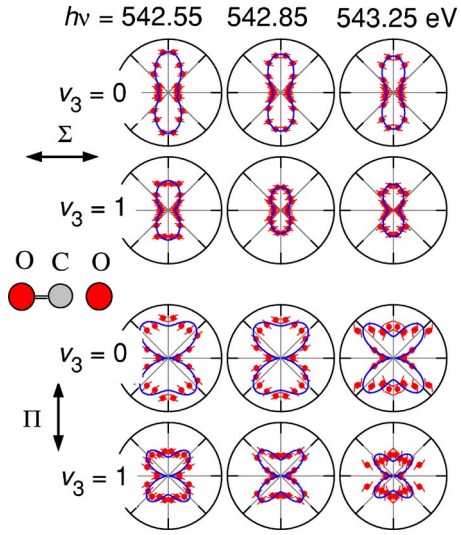

FIG. 3. (Color online) Vibrationally resolved MF-PADs for O 1*s* photoemission from CO_2 aligned parallel (Σ) and perpendicular (Π) to the E vector, measured at photon energies of 542.55, 542.85, and 543.25 eV.

TABLE I. Values of fitted parameters $a_2/a_0, a_4/a_0$, and b_4/b_2.

$h\nu$	$v_3=0$			$v_3=1$		
(eV)	a_2/a_0	a_4/a_0	b_4/b_2	a_2/a_0	a_4/a_0	b_4/b_2
542.55	−1.7(1)	0.9(1)	3.3(3)	−1.1(2)	0.3(1)	5(1)
542.85	−1.6(2)	0.8(1)	3.1(3)	−0.9(3)	0.2(1)	7(1)
543.25	−1.9(1)	1.1(1)	7(1)	−1.1(3)	0.3(1)	6(1)

present MF-PADs are within the plane defined by the molecular axis and the polarization vector E and, thus, correspond to the case of the azimuthal angle $\phi=0$ in the general expression of MF-PADs in [12,13] for the Π channel. To obtain these MF-PADs, we drew the photoelectron spectra, similar to Figs. 2(a) and 2(b), at several angles relative to the molecular axis, analyzed them, and obtained intensities of the individual vibrational components. In addition, we assumed the symmetry property that the MF-PADs are identical in the four quadrants of 90° extension to improve the signal-to-noise ratios. This procedure, however, washes out the asymmetry due to symmetry breaking [22]. The distribution at each energy is normalized so that the integrated intensity for the $v_3=0$ component of the Π channel is unity. The intensities for Σ and Π channels are on relative scales; the intensities for the Σ channels were multiplied by 0.5. The MF-PAD at 542.55 eV summed over all vibrational components are close to those in the previous observations [20,22].

To make a quantitative comparison, we have parametrized the measured MF-PADs. Let us take into account the partial waves up to $l=2$. Then, for the Σ channel, we can express the MF-PADs as

$$I_\Sigma(\theta) = a_0 + a_2 \cos^2\theta + a_4 \cos^4\theta. \quad (1)$$

Here a_0, a_2, and a_4 can be expressed by the complex dipole amplitudes of three waves $s\sigma_g, p\sigma_u$, and $d\sigma_g$ (not shown here). One cannot uniquely determine the ratios of the dipole amplitudes because the three parameters a_0, a_2, and a_4 are described by the four parameters, i.e., the amplitudes of $s\sigma_g, p\sigma_u$, and $d\sigma_g$ and the phase difference between $s\sigma_g$ and $d\sigma_g$. For the Π channel, we can express the MF-PADs as

$$I_\Pi(\theta) = b_2 \sin^2\theta + b_4 \sin^2\theta \cos^2\theta. \quad (2)$$

Here $b_2(\geq 0)$ and $b_4(\geq 0)$ are proportional to the square of the dipole amplitudes for $p\pi_u$ and $d\pi_g$, respectively. The results of the fitting procedure can be seen in Fig. 3. The parameters thus obtained are summarized in Table I.

In case of the Σ channel, variations for different photon energies are within the experimental uncertainties for both $v_3=0$ and $v_3=1$. One may regard this observation as unexpected because the $5\sigma_g$ shape resonance is in this energy range. Indeed this observation sharply contrasts to the result for MF-PADs for core-level photoemission, say from N_2, where MF-PADs are dominated by the f-wave contribution at the shape resonance [8]. The weak energy dependence of MF-PADs for O 1*s* photoemission from CO_2 across the $5\sigma_g$ shape resonance implies that both s and d waves are enhanced at the $5\sigma_g$ resonance of CO_2. We note that the vibra-

tionally averaged MF-PADs gradually vary as a function of energy at higher energies [22]. On the other hand, the parameters given in Table I for $v_3=0$ and 1 are different. The antisymmetric stretching vibration takes place as a result of vibronic coupling (pseudo-Jahn-Teller coupling) which mixes nearly degenerate $1\sigma_g^{-1}$ and $1\sigma_u^{-1}$ states [29]. We note that the coefficients a_i are given by different dipole amplitudes for $v_3=0$ and 1. The difference MF-PADs between $v_3=0$ and 1 may thus suggest the effect of this dynamical vibronic coupling.

The variation of the parameters for the Π channel suggests that the contribution of the d wave increases with the increase in the photon energy. The insufficient quality of the fitting for the MF-PADs of the Π channel implies that the contribution from the f wave is not negligible.

In conclusion, we have reported vibrationally resolved MF-PADs for O $1s$ photoemission from CO_2 at three photon energies close to the O $1s$ $1\sigma_u \rightarrow 5\sigma_g^*$ shape resonance. The measured MF-PADs for the Σ channel do not exhibit variations as a function of photon energy while they depend on the vibrational quantum numbers of the antisymmetric vibrations in the O $1s$ ionized state. A theoretical analysis that takes into account the effect of vibronic coupling caused by antisymmetric vibrations is demanded to understand the present observations.

The experiments were performed at SPring-8 with the approval of the program review committee (2003A0368-NS1-np and 2003B0101-NSb-np). The work was partly supported by the Grants-in-Aid for Scientific Researches from the Japan Society for Promotion of Science and by the Budget for Nuclear Research from Ministry of Education, Science, Sports, Culture and Technology, based on the screening and counseling by the Atomic Energy Commission. We are grateful to the staff of SPring-8 for invaluable help during the experiments.

[1] F. A. Gianturco, M. Guidotti, and U. Lamanna, J. Chem. Phys. **57**, 840 (1972).
[2] V. I. Nefedov, J. Struct. Chem. **11**, 292 (1970).
[3] J. L. Dehmer, D. Dill, and S. Wallace, Phys. Rev. Lett. **43**, 1005 (1979).
[4] K. J. Randall, A. L. D. Kilcoyne, H. M. Köppe, J. Feldhaus, A. M. Bradshaw, J. E. Rubensson, W. Eberhardt, Z. Xu, P. D. Johnson, and Y. Ma, Phys. Rev. Lett. **71**, 1156 (1993).
[5] D. A. Mistrov, A. De Fanis, M. Kitajima, M. Hoshino, H. Shindo, T. Tanaka, Y. Tamenori, H. Tanaka, A. A. Pavlychev, and K. Ueda, Phys. Rev. A **68**, 022508 (2003).
[6] U. Hergenhahn, J. Phys. B **37**, R89 (2004).
[7] D. Dill, J. Chem. Phys. **65**, 5327 (1976).
[8] E. Shigemasa, J. Adachi, M. Oura, and A. Yagishita, Phys. Rev. Lett. **74**, 359 (1995).
[9] F. Heiser, O. Gessner, J. Viefhaus, K. Wieliczek, R. Hentges, and U. Becker, Phys. Rev. Lett. **79**, 2435 (1997).
[10] A. Landers *et al.*, Phys. Rev. Lett. **87**, 013002 (2001).
[11] N. Saito, A. De Fanis, K. Kubozuka, M. Machida, M. Takahashi, H. Yoshida, I. H. Suzuki, A. Cassimi, A. Czasch, L. Schmidt, R. Dörner, K. Wang, B. Zimmermann, V. McKoy, I. Koyano, and K. Ueda, J. Phys. B **36**, L25 (2003).
[12] R. R. Lucchese, J. Electron Spectrosc. Relat. Phenom. **141**, 201 (2004).
[13] D. Dowek, M. Lebech, J. C. Houver, R. R. Lucchese, J. Electron Spectrosc. Relat. Phenom. **141**, 211 (2004).
[14] J. Adachi, K. Hosaka, S. Furuyama, K. Soejima, M. Takahashi, A. Yagishita, S. K. Semenov, and N. A. Cherepkov, Phys. Rev. Lett. **91**, 163001 (2003).
[15] T. Jahnke *et al.*, Phys. Rev. Lett. **93**, 083002 (2004).
[16] K. C. Prince, L. Avaldi, M. Coreno, R. Camilloni, and M. de Simone, J. Phys. B **32**, 2551 (1999).
[17] R. G. Wight and C. E. Brion, J. Electron Spectrosc. Relat. Phenom. **3**, 191 (1974).
[18] M. Schmidbauer, A. L. D. Kilcoyne, H. M. Köppe, J. Feldhaus, and A. M. Bradshaw, Phys. Rev. A **52**, 2095 (1995).
[19] K. Maier, A. Kivimäki, B. Kempgens, U. Hergenhahn, M. Neeb, A. Rüdel, M. N. Piancastelli, and A. M. Bradshaw, Phys. Rev. A **58**, 3654 (1998).
[20] N. Watanabe, J. Adachi, K. Soejima, E. Shigemasa, A. Yagishita, N. G. Fominykh, and A. A. Pavlychev, Phys. Rev. Lett. **78**, 4910 (1997).
[21] J. Adachi, S. Motoki, N. A. Cherepkov, and A. Yagishita, J. Phys. B **35**, 5023 (2002).
[22] N. Saito, K. Ueda, A. De Fanis, K. Kubozuka, M. Machida, I. Koyano, R. Dörner, A. Czasch, L. Schmidt, A. Cassimi, K. Wang, B. Zimmermann, and V. McKoy, J. Phys. B **38**, L277 (2005).
[23] Y. Morishita, Y. Tamenori, M. Machida, M. Oura, H. Yamaoka, M. Suzuki, H. Toyokawa, A. De Fanis, M. Nagoshi, I. Koyano, K. Fujiwara, H. Chiba, G. Pruemper, K. Ueda, I. H. Suzuki, and N. Saito, J. Electron Spectrosc. Relat. Phenom. **144–147**, 255 (2005).
[24] H. Ohashi, E. Ishiguro, Y. Tamenori, H. Kishimoto, M. Tanaka, M. Irie, T. Tanaka, and T. Ishikawa, Nucl. Instrum. Methods Phys. Res. A **467–468**, 529 (2001).
[25] N. Saito, A. De Fanis, I. Koyano, and K. Ueda, J. Electron Spectrosc. Relat. Phenom. **144–147**, 103 (2005).
[26] See http://www.roentdek.com for details on the detectors.
[27] A. Kivimäki, B. Kempgens, K. Maier, H. M. Köppe, M. N. Piancastelli, M. Neeb, and A. M. Bradshaw, Phys. Rev. Lett. **79**, 998 (1997).
[28] P. van der Straten, R. Morgenstern, and A. Niehaus, Z. Phys. D: At., Mol. Clusters **8**, 35 (1988).
[29] W. Domcke and L. S. Cederbaum, Chem. Phys. **25**, 189 (1977).